

Numerical Solutions of Forced Convection Boundary Layer Flow on a Horizontal Circular Cylinder with Newtonian Heating

¹Mohd Zuki Salleh, ²Roslinda Nazar, ^{3,4}Norihan Md Arifin and ⁴Ioan Pop

*¹Faculty of Industrial Science and Technology,
Universiti Malaysia Pahang,
26300 UMP Kuantan, Pahang, Malaysia*

*²Faculty of Science and Technology, Universiti Kebangsaan Malaysia,
43600 UKM Bangi, Selangor, Malaysia*

*³Faculty of Science, Universiti Putra Malaysia,
43400 UPM Serdang, Selangor, Malaysia*

*⁴Institute for Mathematical Research, Universiti Putra Malaysia,
43400 UPM Serdang, Selangor, Malaysia*

*⁵Faculty of Mathematics, University of Cluj,
R-3400 Cluj, CP253, Romania*

E-mail: zukikuj@yahoo.com

ABSTRACT

This study considers the steady forced convection boundary layer flow over a horizontal circular cylinder, generated by Newtonian heating in which the heat transfer from the surface is proportional to the local surface temperature. The governing boundary layer equations are first transformed into a system of non-dimensional equations via the non-dimensional variables, and then into non-similar equations before they are solved numerically using a numerical scheme known as the Keller box method. Numerical solutions are obtained for the skin friction coefficient and the local wall temperature as well as the velocity and temperature profiles.

Keywords: Forced convection, horizontal circular cylinder, Newtonian heating, numerical solution

INTRODUCTION

Boundary layer flow over a circular cylinder was the subject of intense studies since the early work of Prandtl in 1904 (Schlichting (1968)). It is well known that the first solution of the steady forced convection momentum (velocity) boundary layer flow over a circular

cylinder was obtained by Blasius in 1908 (Schlichting (1968)) using the series method. In 1958, Frössling solved also the thermal equation of this problem for the case when the surface temperature of the cylinder is subjected to a constant temperature (Schlichting (1968)). Merkin and Pop (1988) studied the free convection boundary layer on a horizontal circular cylinder with constant heat flux in a viscous fluid, while Ingham and Pop (1987) investigated the free convection about a heated horizontal cylinder embedded in a fluid saturated porous medium. This problem is then extended to viscous and micropolar fluids by many investigators such as Yih (2000), Nazar *et al.* (2002a, 2002b), Ahmad *et al.* (2005) and Molla *et al.* (2005) in various ways. In summary, all of the papers above considered either prescribed wall temperature or prescribed wall heat flux boundary condition. Merkin (1994) has shown that, in general, there are four common heating processes specifying the wall-to-ambient temperature distributions, namely, (i) prescribed wall temperature distributions; (ii) prescribed surface heat flux distributions; (iii) conjugate conditions, where heat is supplied through a bounding surface of finite thickness and finite heat capacity. The interface temperature is not known a priori but depends on the intrinsic properties of the system, namely the thermal conductivity of the fluid and solid, respectively; and (iv) Newtonian heating, where the heat transfer rate from the bounding surface with a finite heat capacity is proportional to the local surface temperature and which is usually termed conjugate convective flow.

Generally, in modelling the convective boundary layer flow problems, the boundary conditions that were usually applied are (i) and (ii). It seems that Merkin (1994) was the first to use the term Newtonian heating for the problem of free convection over a vertical flat. Recently Salleh *et al.* (2009, 2010a, 2010b, 2010c, 2011) and Salleh and Nazar (2010) studied the forced convection boundary layer flow at a forward stagnation point, forced, free and mixed convection boundary layer flow over a horizontal circular cylinder and a solid sphere with Newtonian heating.

The aim of the present paper is to investigate numerically the steady forced convection flow over a horizontal circular cylinder with Newtonian heating. The governing boundary layer equations are first transformed into a system of non-dimensional equations via the non-dimensional variables, and then into non-similar equations before they are solved numerically by the Keller-box method, an implicit finite-difference scheme as described in the books by Cebeci and Bradshaw (1988) and Cebeci and Cousteix (2005).

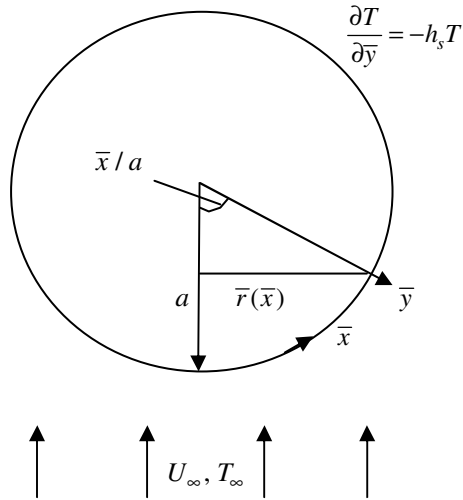


Figure 1: Physical model and coordinate system

PROBLEM FORMULATION

Consider the steady forced convection boundary layer flow and heat transfer of a viscous and incompressible fluid of free stream velocity U_∞ and ambient temperature T_∞ over a horizontal circular cylinder of radius a , which is subjected to a Newtonian heating, as it is shown in Figure 1. It is assumed that the buoyancy forces and the viscous dissipation effects are neglected. Under the boundary layer approximations, the basic dimensional equations are

$$\frac{\partial \bar{u}}{\partial \bar{x}} + \frac{\partial \bar{v}}{\partial \bar{y}} = 0 \quad (1)$$

$$\bar{u} \frac{\partial \bar{u}}{\partial \bar{x}} + \bar{v} \frac{\partial \bar{u}}{\partial \bar{y}} = \bar{u}_e \frac{d\bar{u}_e}{d\bar{x}} + \nu \frac{\partial^2 \bar{u}}{\partial \bar{y}^2} \quad (2)$$

$$\bar{u} \frac{\partial T}{\partial \bar{x}} + \bar{v} \frac{\partial T}{\partial \bar{y}} = \alpha \frac{\partial^2 T}{\partial \bar{y}^2} \quad (3)$$

subject to the boundary conditions (Merkin (1994))

$$\begin{aligned} \bar{u} = \bar{v} = 0, \quad \frac{\partial T}{\partial \bar{y}} = -h_s T \quad \text{at} \quad \bar{y} = 0 \\ \bar{u} \rightarrow \bar{u}_e(\bar{x}), \quad T \rightarrow T_\infty \quad \text{as} \quad \bar{y} \rightarrow \infty \end{aligned} \quad (4)$$

Here $\bar{u}_e(\bar{x}) = 2U_\infty \sin(\bar{x}/a)$, (\bar{u}, \bar{v}) are the velocity components along the (\bar{x}, \bar{y}) axes, T is the local temperature, ν is the kinematic viscosity, α is the thermal diffusivity and h_s is the heat transfer parameter for Newtonian heating.

We introduce now the following non-dimensional variables:

$$\begin{aligned} x = \bar{x}/a, \quad y = \text{Re}^{1/2}(\bar{y}/a), \quad u = \bar{u}/U_\infty, \quad v = \text{Re}^{1/2}(\bar{v}/U_\infty) \\ \theta = (T - T_\infty)/T_\infty, \quad u_e(x) = \bar{u}_e(\bar{x})/U_\infty \end{aligned} \quad (5)$$

where $\text{Re} = U_\infty a / \nu$ is the Reynolds number. Equations (1) – (3) then become

$$\frac{\partial u}{\partial x} + \frac{\partial v}{\partial y} = 0 \quad (6)$$

$$u \frac{\partial u}{\partial x} + v \frac{\partial u}{\partial y} = u_e \frac{du_e}{dx} + \frac{\partial^2 u}{\partial y^2} \quad (7)$$

$$u \frac{\partial \theta}{\partial x} + v \frac{\partial \theta}{\partial y} = \frac{1}{\text{Pr}} \frac{\partial^2 \theta}{\partial y^2} \quad (8)$$

and the boundary conditions (4) become

$$\begin{aligned} u = v = 0, \quad \frac{\partial \theta}{\partial y} = -\gamma(1 + \theta) \quad \text{at} \quad y = 0 \\ \bar{u} \rightarrow u_e(x), \quad \theta \rightarrow 0 \quad \text{as} \quad y \rightarrow \infty \end{aligned} \quad (9)$$

where $\gamma = ah_s \text{Re}^{-1/2}$ represents the conjugate parameter for Newtonian heating. We noticed that (9) gives $\theta = 0$ when $\gamma = 0$, corresponding to having $h_s = 0$ and hence no heating from the cylinder exists. On the other

hand, $u_e(x) = 2 \sin x$ and $Pr = \nu / \alpha$ is the Prandtl number. Further, following Merkin (1994), we look for a solution for this problem of the form

$$\psi = x f(x, y), \quad \theta = \theta(x, y) \quad (10)$$

where ψ is the stream function which is defined as $u = \partial \psi / \partial y$ and $v = -\partial \psi / \partial x$, and this automatically satisfies Equation (6). Using variables (10), Equations. (7) and (8) become

$$\frac{\partial^3 f}{\partial y^3} + f \frac{\partial^2 f}{\partial y^2} + 4 \frac{\sin x \cos x}{x} - \left(\frac{\partial f}{\partial y} \right)^2 = x \left(\frac{\partial f}{\partial y} \frac{\partial^2 f}{\partial x \partial y} - \frac{\partial f}{\partial x} \frac{\partial^2 f}{\partial y^2} \right) \quad (11)$$

$$\frac{1}{Pr} \frac{\partial^2 \theta}{\partial y^2} + f \frac{\partial \theta}{\partial y} = x \left(\frac{\partial f}{\partial y} \frac{\partial \theta}{\partial x} - \frac{\partial f}{\partial x} \frac{\partial \theta}{\partial y} \right) \quad (12)$$

with the boundary conditions

$$\begin{aligned} f = \frac{\partial f}{\partial y} = 0, \quad \frac{\partial \theta}{\partial y} = -\gamma(1 + \theta) \quad \text{at } y = 0 \\ \frac{\partial f}{\partial y} \rightarrow 2 \frac{\sin x}{x}, \quad \theta \rightarrow 0 \quad \text{as } y \rightarrow \infty \end{aligned} \quad (13)$$

It can be easily shown that near the lower stagnation point of the cylinder, $x \approx 0$, Equations (11) and (12) reduce to the following ordinary differential equations:

$$f''' + f f'' + 4 - f'^2 = 0 \quad (14)$$

$$\theta'' + Pr f \theta' = 0 \quad (15)$$

where the prime (') denotes differentiation with respect to y and the boundary conditions are

$$\begin{aligned} f = f' = 0, \quad \theta' = -\gamma(1 + \theta) \quad \text{at } y = 0 \\ f' \rightarrow 2, \quad \theta \rightarrow 0 \quad \text{as } y \rightarrow \infty \end{aligned} \quad (16)$$

In practical applications, the physical quantities of interest are the skin friction coefficient C_f and the wall temperature $\theta_w(x)$, which can be written in non-dimensional form as

$$\text{Re}_x^{1/2} C_f = x \frac{\partial^2 f}{\partial y^2}(x, 0), \quad \theta_w(x) = \theta(x, 0) \quad (17)$$

where $\text{Re} = U_\infty x / \nu$ is the Reynolds number, $C_f = \tau_w / \rho U_\infty^2$ is the skin friction coefficient, with $\tau_w = \mu \left(\frac{\partial \bar{u}}{\partial y} \right)_{y=0}$ is the local wall shear stress and ρ is the fluid density.

THE KELLER BOX METHOD

Finite Difference Scheme

This paper discusses the finite difference scheme on forced convection boundary layer flow over a horizontal circular cylinder, i.e. from Equations (11) and (12) with boundary conditions (13) when $\gamma=1$. We start with introducing new dependent variables $u(x, y)$, $v(x, y)$, $t(x, y)$ and $\theta = s(x, y)$ so that Equations (11) and (12) can be written as

$$f' = u, \quad u' = v, \quad s' = t \quad (18a,b,c)$$

$$v' + f v + 4 \frac{\sin x \cos x}{x} - u^2 = x \left(u \frac{\partial u}{\partial x} - v \frac{\partial f}{\partial x} \right) \quad (18d)$$

$$\frac{1}{\text{Pr}} t' + f t = x \left(u \frac{\partial s}{\partial x} - t \frac{\partial f}{\partial x} \right) \quad (18e)$$

We now consider the net rectangle in the $x - y$ plane shown in Figure 2 and the net points defined as below:

$$\begin{aligned} x^0 &= 0, & x^n &= x^{n-1} + k_n, & n &= 1, 2, \dots, N, \\ y_0 &= 0, & y_j &= y_{j-1} + h_j, & j &= 1, 2, \dots, J, \\ y_J &\equiv y_\infty, \end{aligned}$$

where k_n is the Δx_n -spacing and h_j is the Δy_j -spacing. Here n and j are just the sequence of numbers that indicate the coordinate location, not tensor indices or exponents.

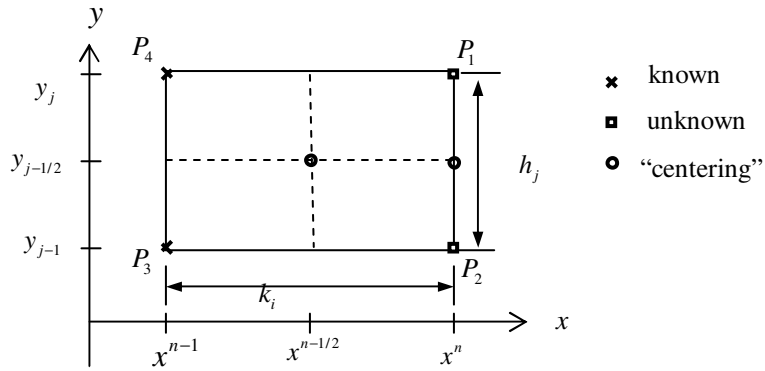


Figure 2: Net rectangle for difference approximations

The derivatives in the x -direction are replaced by finite difference. For example, the finite difference forms for any points are

$$\text{a. } ()_{j-\frac{1}{2}}^n = \frac{1}{2} \left[()_j^n + ()_{j-1}^n \right], \quad ()_j^{n-\frac{1}{2}} = \frac{1}{2} \left[()_j^n + ()_j^{n-1} \right]$$

$$\text{b. } \left(\frac{\partial u}{\partial x} \right)_{j-\frac{1}{2}}^{n-\frac{1}{2}} = \frac{u_{j-\frac{1}{2}}^n - u_{j-\frac{1}{2}}^{n-1}}{k_n}, \quad \left(\frac{\partial u}{\partial y} \right)_{j-\frac{1}{2}}^{n-\frac{1}{2}} = \frac{u_j^{n-\frac{1}{2}} - u_{j-1}^{n-\frac{1}{2}}}{h_j}$$

We start by writing the finite difference form of equations (18a,b,c) for the midpoint $(x^n, y_{j-1/2})$ of the segment P_1P_2 using centered-difference derivatives. This process is called “centering about $(x^n, y_{j-1/2})$ ”. We get

$$f_j - f_{j-1} - \frac{h_j}{2}(u_j + u_{j-1}) = 0 \quad (19a)$$

$$u_j - u_{j-1} - \frac{h_j}{2}(v_j + v_{j-1}) = 0 \quad (19b)$$

$$s_j - s_{j-1} - \frac{h_j}{2}(t_j + t_{j-1}) = 0 \tag{19c}$$

$$\begin{aligned} (v_j - v_{j-1}) + \frac{(1+\alpha)h_j}{4}(f_j + f_{j-1})(v_j + v_{j-1}) + A - \frac{(1+\alpha)h_j}{4}(u_j + u_{j-1})^2 \\ + \frac{\alpha h_j}{2}v_{j-1/2}^{n-1}(f_j + f_{j-1}) - \frac{\alpha h_j}{2}f_{j-1/2}^{n-1}(v_j + v_{j-1}) = (R_1)_{j-\frac{1}{2}} \end{aligned} \tag{19d}$$

$$\begin{aligned} \frac{1}{Pr}(t_j - t_{j-1}) + \frac{(1+\alpha)h_j}{4}(f_j + f_{j-1})(t_j + t_{j-1}) - \frac{\alpha h_j}{4}(u_j + u_{j-1})(s_j + s_{j-1}) \\ + \frac{\alpha h_j}{2}s_{j-1/2}^{n-1}(u_j + u_{j-1}) - \frac{\alpha h_j}{2}u_{j-1/2}^{n-1}(s_j + s_{j-1}) - \frac{\alpha h_j}{2}f_{j-1/2}^{n-1}(t_j + t_{j-1}) \\ + \frac{\alpha h_j}{2}t_{j-1/2}^{n-1}(f_j + f_{j-1}) = (R_2)_{j-\frac{1}{2}} \end{aligned} \tag{19e}$$

where

$$\begin{aligned} (R_1)_{j-\frac{1}{2}} &= -h_j \left[\left(\frac{v_j - v_{j-1}}{h_j} \right) + (1-\alpha)(fv)_{j-\frac{1}{2}} + (\alpha-1)(u^2)_{j-\frac{1}{2}} - A \right] \\ (R_2)_{j-\frac{1}{2}} &= -h_j \left[\frac{1}{Pr} \left(\frac{t_j - t_{j-1}}{h_j} \right) + (1-\alpha)(ft)_{j-\frac{1}{2}} + \alpha(us)_{j-\frac{1}{2}} \right] \\ \alpha &= \frac{x^{n-1/2}}{k_n} \quad \text{and} \quad A = 4 \frac{\sin x \cos x}{x}. \end{aligned} \tag{19f,g,h}$$

We note that $(R_1)_{j-\frac{1}{2}}$ and $(R_2)_{j-\frac{1}{2}}$ involve only the known quantities if we assume that the solution is known on $x = x^{n-1}$. In terms of the new dependent variables, the boundary conditions become

$$\begin{aligned} f(x,0) = 0, \quad t(x,0) = -(1 + s(x,0)) \\ u(x,\infty) = 2 \frac{\sin x}{x}, \quad s(x,\infty) = 0 \end{aligned} \tag{20}$$

Equation (19) are imposed for $j = 1, 2 \dots J$ at given n , and the transformed boundary layer thickness, y_j , is to be sufficiently large so that it is beyond the edge of the boundary layer. The boundary conditions yield at $x = x^n$ are

$$f_0^n = u_0^n = 0, \quad t_0^n = -(1 + s_0^n), \quad u_j^n = 2, \quad s_j^n = 0. \quad (21)$$

Newton's Method

To linearize the nonlinear system of Equation (19) using Newton's method, we introduce the following iterates:

$$\begin{aligned} f_j^{(k+1)} &= f_j^{(k)} + \delta f_j^{(k)}, \quad u_j^{(k+1)} = u_j^{(k)} + \delta u_j^{(k)}, \quad v_j^{(k+1)} = v_j^{(k)} + \delta v_j^{(k)}, \\ s_j^{(k+1)} &= s_j^{(k)} + \delta s_j^{(k)} \quad \text{and} \quad t_j^{(k+1)} = t_j^{(k)} + \delta t_j^{(k)} \end{aligned} \quad (22)$$

Substituting these expressions into Equations (19) and then drop the quadratic and higher-order terms in $\delta f_j^{(k)}$, $\delta u_j^{(k)}$, $\delta v_j^{(k)}$, $\delta s_j^{(k)}$ and $\delta t_j^{(k)}$, this procedure yields the following linear tridiagonal system (we have also dropped the superscript (k) for simplicity):

$$\begin{aligned} \delta f_j - \delta f_{j-1} - \frac{1}{2} h_j (\delta u_j + \delta u_{j-1}) &= (r_1)_j \\ \delta u_j - \delta u_{j-1} - \frac{1}{2} h_j (\delta v_j + \delta v_{j-1}) &= (r_2)_j \\ \delta s_j - \delta s_{j-1} - \frac{1}{2} h_j (\delta t_j + \delta t_{j-1}) &= (r_3)_j \end{aligned} \quad (23)$$

$$\begin{aligned} (a_1)_j \delta v_j + (a_2)_j \delta v_{j-1} + (a_3)_j \delta f_j + (a_4)_j \delta f_{j-1} \\ + (a_5)_j \delta u_j + (a_6)_j \delta u_{j-1} + (a_7)_j \delta s_j + (a_8)_j \delta s_{j-1} &= (r_4)_j \\ (b_1)_j \delta t_j + (b_2)_j \delta t_{j-1} + (b_3)_j \delta f_j + (b_4)_j \delta f_{j-1} \\ + (b_5)_j \delta u_j + (b_6)_j \delta u_{j-1} + (b_7)_j \delta s_j + (b_8)_j \delta s_{j-1} &= (r_5)_j \end{aligned}$$

where

$$(a_1)_j = 1 + \frac{h_j}{2} \left[(1 + \alpha) f_{j-\frac{1}{2}} - \alpha f_{j-\frac{1}{2}}^{n-1} \right], \quad (a_2)_j = (a_1)_j - 2,$$

$$\begin{aligned}
 (a_3)_j &= \frac{h_j}{2} \left[(1 + \alpha)v_{j-\frac{1}{2}} + \alpha v_{j-\frac{1}{2}}^{n-1} \right], & (a_4)_j &= (a_3)_j & (24a) \\
 (a_5)_j &= -\frac{(1 + \alpha)}{2} h_j u_{j-\frac{1}{2}}, & (a_6)_j &= (a_5)_j \\
 (a_7)_j &= (a_8)_j = 0,
 \end{aligned}$$

$$\begin{aligned}
 (b_1)_j &= \frac{1}{\text{Pr}} + \frac{h_j}{2} \left[(1 + \alpha)f_{j-\frac{1}{2}} - \alpha f_{j-\frac{1}{2}}^{n-1} \right], & (b_2)_j &= (b_1)_j - \frac{2}{\text{Pr}} \\
 (b_3)_j &= \frac{h_j}{2} \left[(1 + \alpha)t_{j-\frac{1}{2}} + \alpha t_{j-\frac{1}{2}}^{n-1} \right], & (b_4)_j &= (b_3)_j & (24b)
 \end{aligned}$$

$$\begin{aligned}
 (b_5)_j &= \frac{h_j}{2} \left[-\alpha s_{j-\frac{1}{2}} + \alpha s_{j-\frac{1}{2}}^{n-1} \right], & (b_6)_j &= (b_5)_j \\
 (b_7)_j &= -\frac{h_j}{2} \left[\alpha u_{j-\frac{1}{2}} + \alpha u_{j-\frac{1}{2}}^{n-1} \right], & (b_8)_j &= (b_7)_j
 \end{aligned}$$

and

$$\begin{aligned}
 (r_1)_j &= f_{j-1} - f_j + h_j u_{j-\frac{1}{2}}, & (r_2)_j &= u_{j-1} - u_j + h_j v_{j-1/2} \\
 (r_3)_j &= s_{j-1} - s_j + h_j t_{j-1/2} & & (25)
 \end{aligned}$$

$$(r_4)_j = (R_1)_{j-\frac{1}{2}} - (v_j - v_{j-1}) - h_j \left[(1 + \alpha)f_{j-\frac{1}{2}} v_{j-\frac{1}{2}} - (1 + \alpha) \left(u_{j-\frac{1}{2}} \right)^2 + \alpha v_{j-\frac{1}{2}}^{n-1} f_{j-\frac{1}{2}} - A \right]$$

$$\begin{aligned}
 (r_5)_j &= (R_2)_{j-\frac{1}{2}} - \frac{1}{\text{Pr}} (t_j - t_{j-1}) - h_j \left[(1 + \alpha)f_{j-\frac{1}{2}} t_{j-\frac{1}{2}} - \alpha u_{j-\frac{1}{2}} s_{j-\frac{1}{2}} + \alpha s_{j-\frac{1}{2}}^{n-1} u_{j-\frac{1}{2}} \right] \\
 &+ h_j \left[\alpha u_{j-\frac{1}{2}}^{n-1} s_{j-\frac{1}{2}} + \alpha f_{j-\frac{1}{2}}^{n-1} t_{j-\frac{1}{2}} - \alpha t_{j-\frac{1}{2}}^{n-1} f_{j-\frac{1}{2}} \right]
 \end{aligned}$$

$$[A_j] = \begin{bmatrix} d & 0 & 1 & 0 & 0 \\ -1 & 0 & 0 & d & 0 \\ 0 & -1 & 0 & 0 & d \\ a_6 & a_8 & a_3 & a_1 & 0 \\ b_6 & b_8 & b_3 & 0 & b_1 \end{bmatrix}, \quad d = -\frac{h_j}{2}, \quad 2 \leq j \leq J \quad (28b)$$

$$[B_j] = \begin{bmatrix} 0 & 0 & -1 & 0 & 0 \\ 0 & 0 & 0 & d & 0 \\ 0 & 0 & 0 & 0 & d \\ 0 & 0 & a_4 & a_2 & 0 \\ 0 & 0 & b_4 & 0 & b_2 \end{bmatrix}, \quad d = -\frac{h_j}{2}, \quad 2 \leq j \leq J \quad (29)$$

$$[C_j] = \begin{bmatrix} d & 0 & 0 & 0 & 0 \\ 1 & 0 & 0 & 0 & 0 \\ 0 & 1 & 0 & 0 & 0 \\ a_5 & a_7 & 0 & 0 & 0 \\ b_5 & b_7 & 0 & 0 & 0 \end{bmatrix}, \quad d = -\frac{h_j}{2}, \quad 1 \leq j \leq J-1 \quad (30)$$

$$[\delta_1] = \begin{bmatrix} \delta v_0 \\ \delta t_0 \\ \delta f_1 \\ \delta v_1 \\ \delta t_1 \end{bmatrix}, \quad [\delta_j] = \begin{bmatrix} \delta u_{j-1} \\ \delta s_{j-1} \\ \delta f_j \\ \delta v_j \\ \delta t_j \end{bmatrix}, \quad 2 \leq j \leq J \quad (31)$$

and
$$[r_j] = \begin{bmatrix} (r_1)_{j-\frac{1}{2}} \\ (r_2)_{j-\frac{1}{2}} \\ (r_3)_{j-\frac{1}{2}} \\ (r_4)_{j-\frac{1}{2}} \\ (r_5)_{j-\frac{1}{2}} \end{bmatrix}, \quad 1 \leq j \leq J. \quad (32)$$

To solve Equation (27), we assume that A is nonsingular and it can be factored into

$$[A] = [L][U] \quad (33)$$

where

$$[L] = \begin{bmatrix} [\alpha_1] & & & & \\ [B_2] & [\alpha_2] & & & \\ & & \ddots & & \\ & & & [\alpha_{j-1}] & \\ & & & [B_j] & [\alpha_j] \end{bmatrix} \quad \text{and} \quad [U] = \begin{bmatrix} [I] & [\Gamma_1] & & & \\ & [I] & [\Gamma_2] & & \\ & & & \ddots & \\ & & & & [I][\Gamma_{j-1}] \\ & & & & [I] \end{bmatrix},$$

where $[I]$ is the identity matrix of order 5 and $[\alpha_i]$, and $[\Gamma_i]$ are 5×5 matrices which elements are determined by the following equations:

$$[\alpha_1] = [A_1] \quad (34)$$

$$[A_1] [\Gamma_1] = [C_1] \quad \text{and} \quad (35)$$

$$[\alpha_j] = [A_j] - [B_j][\Gamma_{j-1}], \quad j = 2, 3, \dots, J \quad (36)$$

$$[\alpha_j][\Gamma_j] = [C_j], \quad j = 2, 3, \dots, J-1. \quad (37)$$

Equation (33) can now be substituted into Equation (27), and we get

$$[L][U][\delta] = [r]. \quad (38)$$

If we define $[U][\delta] = [W]$ (39)

then Equation (38) becomes $[L][W] = [r]$ (40)

where

$$W = \begin{bmatrix} [W_1] \\ [W_2] \\ \vdots \\ [W_{J-1}] \\ [W_J] \end{bmatrix}$$

and the $[W_j]$ are 5×1 column matrices. The elements W can be solved from Equation (40)

$$[\alpha_1][W_1] = [r_1] \quad (41)$$

$$[\alpha_j][W_j] = [r_j] - [B_j][W_{j-1}], \quad 2 \leq j \leq J. \quad (42)$$

The step in which Γ_j, α_j and W_j are calculated is usually referred to as the forward sweep. Once the elements of W are found, Equation (39) then gives the solution δ in the so-called backward sweep, in which the elements are obtained by the following relations:

$$[\delta_j] = [W_j] \quad (43)$$

$$[\delta_j^*] = [W_j] - [\Gamma_j][\delta_{j+1}], \quad 1 \leq j \leq J - 1. \quad (44)$$

These calculations are repeated until some convergence criterion is satisfied and calculations are stopped when

$$|\delta v_0^{(i)}| < \varepsilon_1 \quad (45)$$

where ε_1 is a small prescribed value.

RESULTS AND DISCUSSION

The solution starts at $x=0$, with a proper step size Δy , for the interval $0 \leq y \leq y_\infty$ by iteration, then proceeds to the $x > 0$ location with a

proper step size Δx . A solution is considered to converge when the difference between the input and output of the $v(x,0)$ came within 10^{-5} . After obtaining a converged solution, the computation will continue by marching in the x – direction. The step size Δy in y , and the edge of the boundary layer y_∞ had to be adjusted for different values of parameters to maintain accuracy. Therefore, we have used the step size of $\Delta y = 0.02$ and $\Delta x = 0.01$ in the present study.

Equations (11) and (12) subject to the boundary conditions (13) are solved numerically using the Keller-box method with three parameters considered, namely, the Prandtl number Pr , the conjugate parameter $\gamma = 1$ and the coordinate running along the surface of the cylinder, x . In this paper, numerical solutions start at the lower stagnation point of the cylinder, $x \approx 0$, and proceed round the cylinder up to the separation point. For the Prandtl number Pr , it is worth mentioning that small values of Pr ($\ll 1$) physically correspond to liquid metals, which have high thermal conductivity but low viscosity, while large values of Pr ($\gg 1$) correspond to high viscosity oils.

Solving Equation (11) subjects to the corresponding boundary conditions (13), it is found that the separation of the momentum (velocity) boundary layer from the surface of the cylinder takes place at the point $x_s = 104.50^0$, which is in very good agreement with the results reported by Schlichting (1968), Leal (1992) and Ahmad *et al.* (2005). On the other hand, solving Equation (14) subjects to the boundary conditions (16), it is found that there is only a unique value of the reduced skin friction coefficient, $f''(0) = 3.4864$ which is in good agreement with the value $f''(0) = 3.4919$ found by Ahmad *et al.* (2005). We can, thus, conclude that this method works efficiently also for the present problem and we are, therefore, confident that the results presented here are accurate.

Tables 1 and 2 present the values of $\theta_w(x)$, $\frac{\partial^2 f}{\partial y^2}(x,0)$ and $f(x,\infty)$ obtained by solving Equations (11) and (12) subject to boundary conditions (13) and the values of the reduced skin friction coefficient $\frac{\partial^2 f}{\partial y^2}(x,0)$ at some positions x for $Pr = 7$ and 10 when $\gamma = 1$,

respectively. It is noticed from Table 1 that the values of the wall temperature are sensitive to the small changes in Pr. For example, as Pr increases, the value of the wall temperature $\theta_w(x)$ decreases. On the other hand, it is seen from Table 2 that due to the decoupled boundary layer equations (11) and (12), there is only a unique value of the reduced skin friction $\frac{\partial^2 f}{\partial y^2}(x,0)$ for all values of Pr at different positions x until separation takes place. The reduced skin friction coefficient decreases as the position x increases around the cylinder.

TABLE 1: Values of $\theta_w(x)$, $\frac{\partial^2 f}{\partial y^2}(x,0)$ and $f(x,\infty)$ for Pr = 7 and 10, obtained by solving Equations (11) - (13) when $\gamma = 1$

Pr x	$\theta_w(x)$	
	7	10
0	1.4511	1.0704
0.2	0.9153	0.5371
0.4	0.7519	0.3548
0.6	0.6741	0.2599
0.8	0.6440	0.2091
1.0	0.6497	0.1872
1.2	0.6930	0.1915
1.4	0.7896	0.2283
1.6	0.9935	0.3251
1.8	1.7549	0.7209
$\frac{\partial^2 f}{\partial y^2}(x,0)$	3.4864	3.4864
$f(x,\infty)$	11.0742	11.0742

TABLE 2: Values of the reduced skin friction coefficient $\frac{\partial^2 f}{\partial y^2}(x,0)$ at some positions x when $\gamma = 1$

x	0	0.2	0.4	0.6	0.8	1.0	1.2	1.4	1.6	1.8
x_0	0^0	11.46^0	22.92^0	34.38^0	45.84^0	57.30^0	68.75^0	80.21^0	91.67^0	103.13^0
$\frac{\partial^2 f}{\partial y^2}(x,0)$	3.4864	3.4293	3.2661	3.0056	2.6601	2.2462	1.7825	1.2858	0.7646	0.1437

Figure 3 displays the velocity profiles $\frac{\partial f}{\partial y}$ near the lower stagnation point of the cylinder, $x \approx 0$, when $\gamma = 1$ for the present results and those reported by Ahmad *et al.* (2005). This figure shows that the present results are in good agreement with the previously published results.

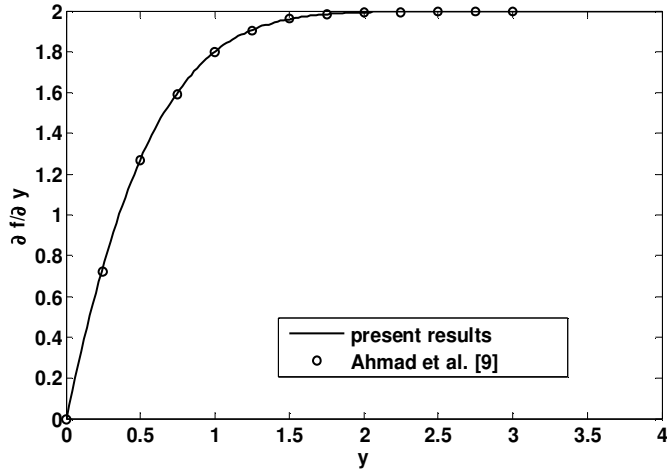


Figure 3: Velocity profiles $\frac{\partial f}{\partial y}(x, y)$ near the lower stagnation point of the cylinder, $x \approx 0$ when $\gamma = 1$

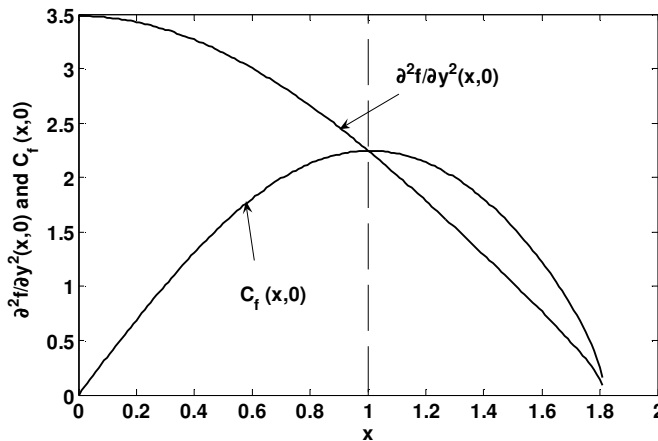


Figure 4: Variation of the reduced skin friction $\frac{\partial^2 f}{\partial y^2}(x, 0)$ and the skin friction coefficient

$$C_f(x, 0) \text{ when } \gamma = 1$$

Figure 4 illustrates the variation of the reduced skin friction $\frac{\partial^2 f}{\partial y^2}(x,0)$ and the skin friction coefficient $C_f(x,0)$. From these figures, it is found that we have only a unique graph of $\frac{\partial f}{\partial y}$, $\frac{\partial^2 f}{\partial y^2}(x,0)$ and $C_f(x,0)$ for all values of Pr, due to the decoupled Equations (11) and (12).

Figure 5 presents the temperature profiles near the lower stagnation point of the cylinder, $x \approx 0$, for Pr = 7 and 10 when $\gamma = 1$. It can be seen that as Pr increases, the temperature profiles decrease and the thermal boundary layer thickness also decreases. This is because for small values of the Prandtl number Pr ($\ll 1$) the fluid is highly conductive. Physically, if Pr increases, the thermal diffusivity decreases and this phenomenon lead to the decreasing of energy transfer ability that reduces the thermal boundary layer.

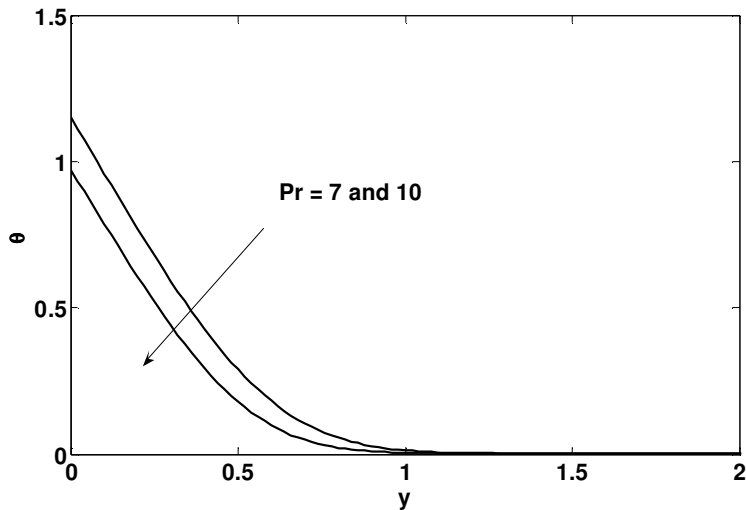


Figure 5: Temperature profiles $\theta(x, y)$ near the lower stagnation point of the cylinder, $x \approx 0$, for values of Pr = 7 and 10 when $\gamma = 1$

Figure 6 illustrates the variation of wall temperature $\theta(x,0)$ with Prandtl number Pr when $\gamma = 1$. To get a physically acceptable solution, Pr must be greater than or equals to a critical value of Pr , say Pr_c , depending on γ . It can be seen from this figure that $\theta(x,0)$ becomes large as Pr approaches the critical value $Pr_c = 1.7519$ when $\gamma = 1$. From Equation (12), we obtain

$$\frac{\partial^2 \theta}{\partial y^2} = 0 \quad (46)$$

for small values of Pr ($\ll 1$). Solving this equation with the boundary conditions (13) and with $\theta(x_0) = 0$, we get

$$\theta(y) = -y \quad (47)$$

when Pr small ($\ll 1$) and near x_0 (x_0 refers to x in degrees). This relation shows that near the point x_0 the temperature becomes negative for small values of the Prandtl number and this is not physically realizable. However, for larger values of the Prandtl number, namely $Pr = 7$ and 10 , the temperature of the thermal boundary layer does not diminish at the surface of the cylinder.

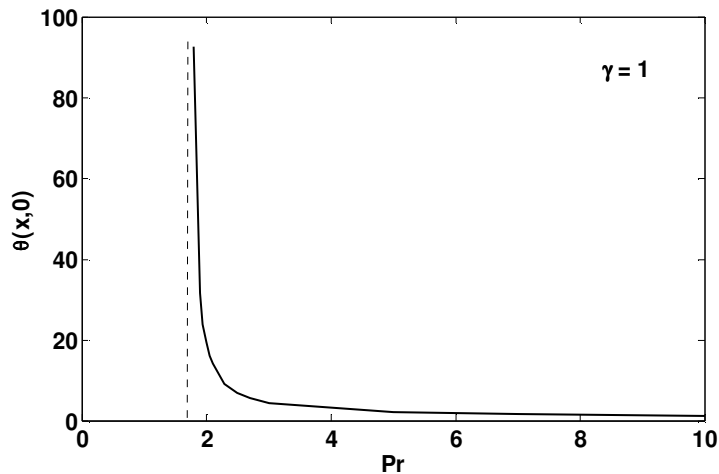


Figure 6: Variation of the wall temperature $\theta(x,0)$ with Prandtl number Pr when $\gamma = 1$

Figure 7 illustrates the variation of the wall temperature $\theta(x,0)$ with conjugate parameter γ when $Pr = 7$ and 10 . Also, to get a physically acceptable solution, γ must be less than or equal to a critical value of γ , say γ_c , depending on Pr . It can be seen from this figure that $\theta(x,0)$ becomes large as γ approaches the critical values $\gamma_c = 1.0353$ and 1.5167 when $Pr = 7$ and 10 , respectively.

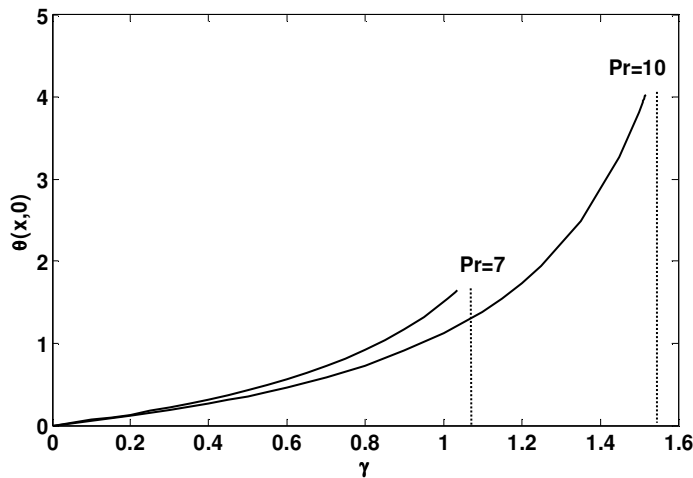


Figure 7: Variation of the wall temperature $\theta(x,0)$ with conjugate parameter γ when $Pr = 7$ and 10

CONCLUSIONS

In this paper, we have numerically studied the problem of forced convection boundary layer flow over a horizontal circular cylinder with Newtonian heating condition. It is shown in this paper how the Prandtl number Pr and the parameter conjugate γ affect the temperature profiles and also the position of the temperature profiles around the surface of the cylinder where it diminishes. We can conclude that

- an increase in the value of Pr leads to a decrease in temperature profiles
- to get a physically acceptable solution, Pr must be greater than or equal to Pr_c (critical value of Pr) depending on γ , and also, γ

must be less than or equal to γ_c (critical value of γ) depending on Pr

- the separation of the momentum boundary layer from the surface of the cylinder takes places at the point $x_s = 104.50^0$ for all values of Pr and γ .

ACKNOWLEDGEMENTS

The authors gratefully acknowledge the financial supports received from the Universiti Kebangsaan Malaysia (UKM-ST-07-FRGSS0036-2009) and research grant from the Universiti Malaysia Pahang (RDU090308).

REFERENCES

- Ahmad, S., Nazar, R.M. and Pop, I. 2005. Forced convection boundary layer flow over a horizontal circular cylinder with constant surface heat flux. *Prosiding Simposium Kebangsaan Sains Matematik ke XIII, Kedah, Malaysia, 31 May - 2 June 2005*.
- Cebeci, T. and Cousteix, J. 2005. *Modeling and Computation of Boundary-Layer Flows: Laminar, Turbulent and Transitional Boundary Layers in incompressible and Compressible Flow*. New York: Springer Berlin Heidelberg,.
- Cebeci, T. and Bradshaw, P. 1988. *Physical and Computational Aspects of Convective Heat Transfer*. New York: Springer.
- Ingham, D.B. and Pop, I. 1987. Natural convection about a heated horizontal cylinder in porous medium. *Journal of Fluid Mechanics*. **184**: 157-181.
- Leal, L.G. 1992. *Laminar Flow and Convective Transport Processes: Scaling Principles and Asymptotic Analysis*. London: Butterworth-Heinemann.
- Merkin, J.H. 1977. Mixed convection from a horizontal circular cylinder. *International Journal of Heat and Mass Transfer*. **20**: 73-77.

- Merkin, J.H. and Pop, I. 1988. A note on the free convection boundary layer on a horizontal circular cylinder with constant heat flux. *Warme- und Stoffubert.* **22**: 79-81.
- Merkin, J.H. 1994. Natural convection boundary-layer flow on a vertical surface with Newtonian Heating. *International Journal of Heat and Fluid Flow.* **15**: 392-398.
- Mola, M.M., Hossain, M.A. and Gorla, R.S.R. 2005. Natural convection flow from an isothermal horizontal circular cylinder with temperaturw dependent viscosity. *Heat and Mass Transfer.* **41**: 594-598.
- Nazar, R., Amin, N. and Pop, I. 2002a. Mixed convection boundary layer flow from a horizontal circular cylinder with a constant surface heat flux. *Heat and Mass Transfer.* **40**: 219-227.
- Nazar, R., Amin, N. and Pop, I. 2002b. Free convection boundary layer on an isothermal horizontal circular cylinder in a micropolar fluid. *Heat Transfer 2002, Proceedings of the Twelfth International Heat Transfer Conference.* 525-530.
- Salleh, M.Z., Nazar, R. and Pop, I. 2009. Forced convection boundary layer flow at a forward stagnation point with Newtonian heating. *Chemical Engineering Communications.* **196**: 987-996.
- Salleh, M.Z. and Nazar, R. 2010. Free convection boundary layer flow over a horizontal circular cylinder with Newtonian heating. *Sains Malaysiana.* **39**(4): 671-676.
- Salleh, M.Z., Nazar, R. and Pop, I. 2010a. Mixed convection boundary layer flow over a horizontal circular cylinder with Newtonian heating. *Heat and Mass Transfer.* **46**(1): 1411-1418.
- Salleh, M.Z., Nazar, R. and Pop, I. 2010b. Modeling of free convection boundary layer flow on a solid sphere with Newtonian heating. *Acta Applicandae Mathematicae.* **112**: 263-274.
- Salleh, M.Z., Nazar, R. and Pop, I. 2010c. Mixed convection boundary layer flow about a solid sphere with Newtonian heating. *Archives of Mechanics.* **62**(4): 283-303.

Numerical Solutions of Forced Convection Boundary Layer Flow on a Horizontal Circular Cylinder with Newtonian Heating

- Salleh, M.Z., Nazar, R., Arifin, N.M., Pop, I. and Merkin, J.H. 2011. Forced convection heat transfer over a horizontal circular cylinder with Newtonian heating, *Journal of Engineering Mathematics*. **69**(1): 101-110.
- Schlichting, H. 1968. *Boundary Layer Theory (6th edition)*. New York: Mc-Graw-Hill Inc.
- Yih, K.A. 2000. Effect of uniform blowing/suction on MHD-natural convection over a horizontal cylinder: UWT or UHF. *Acta Mechanica*. **144**: 17-27.